



EUROfusion

EUROFUSION WPJET1-PR(14) 12725

S Brezinsek et al.

Beryllium Migration in JET ITER-like Wall Plasmas

Preprint of Paper to be submitted for publication in
Nuclear Fusion



This work has been carried out within the framework of the EUROfusion Consortium and has received funding from the Euratom research and training programme 2014-2018 under grant agreement No 633053. The views and opinions expressed herein do not necessarily reflect those of the European Commission.

This document is intended for publication in the open literature. It is made available on the clear understanding that it may not be further circulated and extracts or references may not be published prior to publication of the original when applicable, or without the consent of the Publications Officer, EUROfusion Programme Management Unit, Culham Science Centre, Abingdon, Oxon, OX14 3DB, UK or e-mail Publications.Officer@euro-fusion.org

Enquiries about Copyright and reproduction should be addressed to the Publications Officer, EUROfusion Programme Management Unit, Culham Science Centre, Abingdon, Oxon, OX14 3DB, UK or e-mail Publications.Officer@euro-fusion.org

The contents of this preprint and all other EUROfusion Preprints, Reports and Conference Papers are available to view online free at <http://www.euro-fusionscipub.org>. This site has full search facilities and e-mail alert options. In the JET specific papers the diagrams contained within the PDFs on this site are hyperlinked

Beryllium Migration in JET ITER-like Wall Plasmas

S. Brezinsek¹, A. Widdowson², M. Mayer³, V. Philipps¹, P. Baron-Wiechec², J.W. Coenen¹, K. Heinola⁴, A. Huber¹, J. Likonen⁴, P. Petersson⁵, M. Rubel⁵, M.F. Stamp², D. Borodin¹, J.P. Coad², A.G. Carrasco⁵, A. Kirschner¹, S. Krat³, K. Krieger³, B. Lipschultz², Ch. Linsmeier¹, G.F. Matthews², K. Schmid³ and JET contributors^{*}

EUROfusion Consortium, JET, Culham Science Centre, Abingdon, OX14 3DB, UK

¹Institut für Energie- und Klimaforschung - Plasmaphysik, Forschungszentrum Jülich, 52425 Jülich, Germany

²CCFE Fusion Association, Culham Science Centre, Abingdon, OX143DB, UK

³Max-Planck-Institut für Plasmaphysik, D-85748 Garching, Germany

⁴TEKES, VTT, PO Box 1000, 02044 VTT, Espoo, Finland

⁵Royal Institute of Technology (KTH), Association VR, 100 44 Stockholm, Sweden

Corresponding Author: sebastijan.brezinsek@jet.efda.org

^{*}See the Appendix of F. Romanelli et al., Proceedings of the 25th IAEA Fusion Energy Conference 2014, Saint Petersburg, Russia

Abstract:

The understanding of material migration is a key issue for a successful and safe operation of ITER. JET is used as test bed to investigate the process cycle which is connected the lifetime of first wall components by erosion and the safety due to long-term retention. Divertor configuration: The current understanding of Be migration in the JET-ILW can be described as follows. Neutral Be and BeD from physical and chemical assisted physical sputtering by CX neutrals and residual plasma flux at the recessed wall enters the plasma, is dissociated, ionised and transported by SOL-flows towards the inner divertor where significant deposition takes place. The amount of Be eroded at the first wall and the amount of Be deposited in the inner divertor are in fair agreement (21 – 28g) though the balance is yet incomplete due limited analysis of PFCs components both in divertor and main chamber. However, comparing equal sets of PFCs components, the primary impurity source in JET-ILW is by a factor 5.3 reduced in comparison with JET-C resulting in a lower divertor material deposition by more than an order of magnitude. Within the divertor, Be performs much less re-erosion and transport steps than C due to an energetic threshold for Be sputtering and inhibits by this the transport to the divertor floor and to remote areas at the pump-duct entrance. The overall low migration is also consistent with the low fuel inventory and dust production ($< 1g$) with the JET-ILW. Moreover, it can explain that the inner divertor target plates, which remains at the strike-line without net-deposition, represents a permanent tungsten erosion zone in contrast to thick deposits in the case of C and JET-C. Limiter configuration: Be gross erosion at the contact point was in-situ determined by spectroscopy between 4% ($E=35eV$) and above 100% caused by Be self-sputtering ($E = 200eV$). Chemical assisted physical sputtering via BeD has been identified to contribute to the effective Be sputtering yield, i.e. at $E = 75eV$ about 1/3 enhanced erosion with respect to bare physical sputtering. An effective gross yield of 10% represents a representative yield for limiter plasma conditions in the initial campaign. This is equivalent to an average erosion rate of $4.1 \times 10^{18} Bes^{-1}$ or 1.5g Be sputtered from one mid plane tile. The corresponding net erosion rate deduced from tile profiling - amounts $2.3 \times 10^{18} Bes^{-1}$ if normalized to the total limiter time. This is equivalent to 0.8g Be revealing a factor two between net and

gross erosion. The primary impurity source in limiter configuration in JET-ILW is only 25% above the JET-C case. The main fraction of eroded Be stays within the main chamber and only a small fraction of neutral Be escapes geometrically from the main chamber into the divertor.

1 Introduction

The understanding of material migration, thus the process cycle of material erosion, transport and deposition is one of the key issues for a successful and safe operation of the ITER tokamak and a future fusion reactor. This process cycle is associated with the lifetime of first wall material components, the so-called plasma-facing components PFCs, by erosion, and with the safety aspect due to long-term tritium retention. The latter is both in current fusion devices as well as in ITER dominated by co-deposition of tritium [1]. Most of the present knowledge is based on tokamaks with carbon-based first wall materials and in-situ information obtained from optical spectroscopy during plasma operation and combined with detailed post-mortem analysis after extraction of PFCs. In the common understanding, the main chamber is identified as primary erosion source and material is transport via scrape-off layer (SOL) flows in normal magnetic field configuration predominantly towards the inner divertor region where finite material deposition occurs [2]. In a subsequent multistep process, material transport to remote and inaccessible areas takes place which led to the abandon of carbon as plasma-facing material due unacceptable high fuel retention content in co-deposited layers and inhibits safe conditions for ITER [3]. The outer divertor, though net-erosion zone, plays only a minor role in the overall large material transport which can reach g levels of migrating material for typical current day devices. Predictions to ITER and fusion reactors are based on this physics understanding and the adaption of the appropriate material selection is done with the aid of plasma-wall interaction codes such as ERO [4] or WallDYN [5]. The exchange of PFCs as in ASDEX-Upgrade from graphite to full tungsten [6] and recently in JET from carbon-fibre composite to beryllium (Be main chamber) and W (W divertor) [7] provides the ideal test bed to verify the physics assumptions. Indeed both devices demonstrated a reduction in fuel retention and transport to remote areas, which underlined that with carbon, chemical erosion at low or thermal impact energy (ions and neutrals) dominated the material migration cycle.

Details about the residual carbon content in the JET-ILW are described in sec. **2**, beryllium erosion and transport in limiter configuration are presented in sec. **3** and in divertor configuration in sec. **4**. The overall migration in JET-ILW, differences with respect to JET-C, and the physics mechanisms responsible for the vast reduction of migration, as well as the absence of net-deposition at the inner divertor strike-line area, are given in **5**. Brief conclusions drawn for ITER from JET and a summary (sec. **6**) couplets this contribution.

2 Residual C-content in JET-ILW operational regimes

The carbon (C) content in the plasma edge dropped after installation of the JET-ILW by about a factor 20 in the diverted plasma phase of discharges throughout the first

year of operation, labelled as C28-C30, and prior to the exchange of selected PFC tiles [8]. Apart from an initial clean-up phase, the plasma operation can be described as virtually carbon-free, whereas the residual C from the clean-up is found at net-deposition zones like the divertor floor [19]. The overall C reduction remained low and one order of magnitude below the values in JET-C in the second year of JET-ILW operation after the tile intervention, labelled as C31-C33, as shown in fig. 1. Fig. 1 describes statistically the plasma edge content in the main chamber during the divertor phase in all discharges performed in deuterium with the JET-ILW. Monitoring discharges with identical plasma shape and operational parameters have been regularly executed to document the change of the impurity content, thus primarily the residual C levels, and the migrating Be in the JET vessel by optical spectroscopy [8]. Fig. 2 shows for the inner and outer divertor the flux ratio of CII (515nm), representing primarily the re-eroded/reflected C flux, over $D\gamma$, representing the recycling flux, as well as the flux ratio of $BeII$ (528nm), representing primarily the re-eroded/reflected Be flux, over $D\gamma$. The flux ratios are providing a good measure of the divertor impurity status and the lower envelope reveals almost constant conditions in C and Be in the first year of operation after an initial clean-up phase of C and a build-up phase of Be [15]. However, a slight increase of the C content in the outer divertor of less than 50% in the period C33 with respect to the minimum C values in JET-ILW in C28 has been detected and can be seen in fig. 2b. The reason for the increase is mainly caused by the exposure of back-sides of divertor CFC tiles by high neutral deuterium flux which are not coated by W, by the release of C present in-situ in the W coating due to the manufacturing process, by C resulting from air leaks as well as at high input power and low density operation by potential damage of the W-coatings. Fig. 2a shows also that at the end of the second year of operation a slight reduction of the Be base level (lower envelope) in the inner divertor took place which is likely a consequence of plasma operation at higher divertor electron temperatures in high performance H-mode plasmas prior to the execution of the standard monitor discharges. The post-mortem results presented here are from the first tile intervention following the operational period of almost constant divertor impurity conditions (C28-C30) where all W-coated CFC divertor tiles were in-tact, thus, the JET-ILW was presenting ultimately a tokamak with Be/W PFCs - a good test bed for ITER [9].

However, JET with its inertial cooled PFCs and the inductive-pulsed operation is limited in discharge duration; the typical ratio between operational time in limiter and divertor configuration per discharge is about 1:3. Moreover, in the initial JET-ILW exploitation (2011-2012) a significant portion of the total plasma time (19h) was devoted to limiter operation (6h) which can be compared with 33h plasma time in divertor and 12h in limiter configuration in the last JET-C operation period (2008-2009) [10]. Separation of the two operational regimes is required in order to describe the material migration cycle in JET-ILW by optical spectroscopy and post-mortem analysis of components.

3 Limiter configuration operation with the JET-ILW

JET operation in limiter configuration was conducted to qualify the design of the castellated massive Be PFCs, to determine the Be sputtering yield, and by this to verify the ERO code and available atomic data; ERO is applied for lifetime predictions of first

wall Be components in ITER [25]. In dedicated inner-wall limited discharges, the local plasma conditions at the inboard limiters as well as the deuteron impact energies were varied in the range of $35 - 200\text{eV}$ by deuterium fuelling. The effective sputtering yield for Be gross erosion at the limiter contact point was in-situ determined by optical emission spectroscopy, observing $BeII$ and D_γ , to be between 4.0% and 20% due to predominant deuteron impact, and finally more than 100% due to Be self-sputtering (fig. 3a) [12]. The measured yields are effective as they are averaged over the observation chord at the limiter contact point which compromises variation of impinging fluxes, impact angles, surface temperatures and plasma conditions. Therefore, these effective Be yields were compared with ERO calculations considering these variations and providing synthetic diagnostic views to benchmark the code and its input data directly with the spectroscopic measurements. ERO calculations overestimate the effective Be yield by about a factor 2 which can be partially explained by shadowing of neighboured limits [11].

The effective erosion yields are also about a factor 2 larger than effective C erosion yields in JET-C whereas less impact of self-sputtering in the C case occurs at the high energy end. At the accessible low energy end in the limiter discharges, the yield is lower though chemical assisted physical sputtering (CAPS) of Be via BeD has been identified to contribute to the effective sputtering yield, i.e. at impact energies of 75eV and $T_{Be_{base}} = 200^\circ\text{C}$ about 1/3 enhanced erosion with respect to normal physical sputtering as shown in fig. 3b [12]. The appearance of CAPS acts as an additional sputtering channel, but requires a certain amount of deuterium to be presented on the top-most interaction layer. As the deuterium content decreases with surface temperature, the impact of CAPS on the total Be sputtering yield decreases with surface temperatures and vanishes at $T_{Be_{base}} \simeq 520^\circ\text{C}$. The release of BeD can be in form of BeD_x with $x = 1, 2, 3$, whereas only BeD was experimentally observed by optical emission spectroscopy. With increase of $T_{Be_{base}}$, D_2 is directly desorbed from the Be surface reducing the deuterium content in the interaction layer and causing the decrease of BeD emission whereas the deuterium recycling flux remained constant [12]. Indeed the contribution of CAPS to the total effective Be sputtering yield observed in JET at $E_n = 75\text{eV}$ is in-line with experimental results in PISCES-B [26] where CAPS was observed before and studied as function of biasing temperature of the Be target plate as shown in fig. 3c). Molecular Dynamics is capable to reproduce the fraction of Be erosion sputtered via CAPS [27], but is not yet in agreement with the surface temperature dependence observed in JET. CAPS is currently in the process to be implemented in ERO which will increase the confidence in the ITER predictions. It should be noted, that CAPS gains importance over classical physical sputtering at low impact energies (fig. 3c), however, as the process is physically driven, a minimum energy is required to sputter the Be which is in vast contrast to chemical erosion of C where even thermal deuterons can induce chemical erosion via methane etc. [28]

In a first approximation, deduced from spectroscopic measurements of $BeII$, thus Be^+ which is unaffected of the initial beryllium sputtering process, an effective gross yield of 10% can be estimated to be the representative yield for the averaged limiter plasma conditions in the initial JET-ILW campaign. This results in an average Be erosion rate of $4.1 \times 10^{18} \text{Bes}^{-1}$ or 1.5g Be sputtered from one limiter tile ($A_{tile} = 0.025\text{m}^2$) in the view of the spectroscopic system (observation chord in fig. 5a with $A_{spot} = 0.011\text{m}^2$) in the first year of operation. Post-mortem analysis of Be tiles of the inboard limiters (fig. 5b)

provided information on the campaign averaged Be erosion rate by different techniques (profilometry, NRA, RBS) [10, 13, 14]. The net erosion rate for one mid plane Be tile deduced from tile profiling - amounts $2.3 \times 10^{18} \text{Bes}^{-1}$ if one considers the normalization to the total limiter exposure time in the campaign. This is equivalent $0.8g$ Be resulting from one mid plane tile which can be compared with spectroscopy. Comparison of the net erosion with the corresponding tile in JET-C and normalization to the operational time reveals a higher erosion rate in the JET-ILW case, however, taking into account the different number of interacting limiters in JET-C (#16) and JET-ILW (#10) reduces the discrepancy. The primary impurity source in limiter configuration in JET-ILW is only 25% above the JET-C case. This is in good agreement with the spectroscopic observations, considering that some erosion of the limiters takes also place in the diverted plasma phase and that gross vs. net erosion is compared.

For the total Be source estimation both, spectroscopy and post-mortem analysis, must extrapolate the local information to the total limiter interaction area which represents a fraction of the total inner wall protruding limiters ($A_{lim}^{HFS} = 4.5m^2$). Additional measurements were obtained on the top and bottom tiles of the high-field side (HFS) poloidal limiter rail showing the peak erosion in the centre and almost negligible erosion at the other areas. Interpolation in poloidal direction and extrapolation to all toroidal limiters results in an estimation of the total Be erosion of about $8g$ in the first year of ILW operation. Apart from dedicated experiments, limiter operation is required in the ramp-up and ramp-down phase in all JET-ILW discharges connecting plasmas to the HFS and low-field side (LFS) limiters. Post-mortem analysis revealed that the erosion on the LFS limiters is poloidally asymmetric [13] with stronger erosion at the lower half of the limiter rail with the maximum at the centre. This centre tile showed Be erosion of at least $10\mu m$ - erasing a Ni marker layer which challenges absolute quantification on the LFS. Further erosion has been observed in protection tiles which need to be taken into the calculation in future as well as the massive upper dump plate made of Be which has been partially molten due to disruptions - which makes the erosion determination challenging. The main chamber erosion of C in JET-C was previously estimated [14] to be amount $237g$ of C, but with a twice as long operational time in the erosion-dominated limiter phase.

The main fraction of Be eroded at the limiters in limiter configuration stays within the main chamber (fig. 5c), mostly deposited in recessed areas like the limiter wings and partially on the wall cladding; only a small fraction of neutral Be escapes geometrically from the main chamber into the divertor entrance and can be there deposited. Indeed the initial JET-ILW experiment in diverted configuration identified moderate surface coverage of W by Be [15] after $625s$ in limiter configuration. However, the amount entering the divertor is insignificant in comparison with Be transported into the divertor in x-point plasmas with strike lines positioned on the target plates.

4 Divertor configuration operation with the JET-ILW

With the full W divertor installed in the JET-ILW, no PFCs made of the main chamber wall material are used in the divertor, thus, all Be ions flowing into the divertor and causing potentially W sputtering are originated primarily in the main chamber during diverted plasma operation. Fig. 4 shows the change in the effective Be sputtering yield in the main

chamber during the different phases of the monitoring discharge mentioned before and described in [29]: limiter phase, ohmic divertor phase, L-mode phase and H-mode phase. The effective Be sputtering yield drops strongly due the fact that a) the limiter phase is in the Be self sputtering regime, b) the impact energy of impinging ions drops from limiter to divertor phase due to the cold SOL plasma, and c) the confinement of the particles in the plasma increase. The total Be source can be estimated by appropriate multiplication with the Be surface interaction area as described below. Thereby, homogenous Be and BeD emission in toroidal and poloidal direction at the inner wall can be measured by spectroscopy resulting from erosion processes in these recessed areas. The origin of these processes is twofold: energetic charge exchange neutrals (CXN) and residual plasma flux are impinging the recessed wall area ($A_{wall}^{HFS} = 18.5m^2$) equipped primarily by Be-coated inconel cladding tiles ($A_{clad}^{HFS} = 11.2m^2$ of which 2/3 is Be and the rest protective W tiles) between poloidal limiters which are located typically between 6cm and 10cm behind the separatrix. Horizontal movement of the plasma column by several cm, thus variation of the distance to the Be surface of the same degree, is causing variations of the Be and BeD flux indicating that the low energetic deuterium ion flux contributes significantly to the erosion of the Be cladding.

Dedicated Be long-term samples (sachet samples) installed at different poloidal and toroidal locations between the cladding tiles prior to the first ILW plasma were replaced after the first year of operation for post-mortem analysis. All probes show measurable erosion [16] confirming that the Be cladding is a zone of net erosion as well as the limiters which are about 2cm closer to the plasma, but still deep in the SOL. Quantification of the erosion was performed by RBS providing a local Be erosion rate of $0.78 \times 10^{18} Bm^{-2}s^{-1}$ when normalized to the total operational time. This results in a net erosion of 12.2g of Be from the whole inner wall in the integrated divertor time of the first ILW campaign. This rate can directly be compared with the erosion rate of $3.14 \times 10^{19} Cm^{-2}s^{-1}$ obtained in the operational phase 2005-2009 in JET-C where similar long-term samples were installed and analysed [17]. This is a significant difference by a factor of 4.0. The ratio between the total sputtering yield of Be and C gets even larger and amounts 5.3 when the different total area of CFC cladding in JET-C to Be cladding in JET-ILW is considered. The CXN fluxes and the residual plasma flux impinging on the first wall are in both JET PFC configurations similar, a difference in the involved erosion processes is required to explain the difference in the primary impurity source. Indeed this difference can be solely explained by chemical erosion of C at the lowest, even thermal impinging energies of deuterium. Though CAPS in the case of Be has been observed, the process is different to the thermally activated chemical erosion of C, as a clear energetic threshold at about 10eV energy exists which inhibits the erosion below this minimum required damage energy. The reduction of the impurity concentration in the plasma edge and the primary erosion source is also consistent with the reduction of the C content observed in JET-C in He plasmas. In both cases, the JET-ILW case with D plasma and the JET-C case with He plasma, the fundamental process of chemical erosion at low impact energies is absent and can explain the drop in the impurity content which is then reflected in the corresponding values of Z_{eff} in the plasma core ($Z_{eff} = 1.2$ in JET-ILW D, $Z_{eff} = 2.5$ in JET-C He and $Z_{eff} = 2.0$ in JET-C in D plasmas) [9].

The total main chamber Be source in diverted configuration includes also Be eroded from

the low field side. However, in contrast to the high field side, no outer wall Be cladding exists which can be bombarded by CXN and residual plasma flux. Thus, the outer wall Be source in diverted configuration is given by the poloidal limiters which are typically 4 – 8cm away from the separatrix, thus, closer than the inner wall cladding. The measured erosion of limiters, mentioned in the previous section, is partially caused by CXN, by residual plasma flux and potentially by enhanced filamentary transport [18]. An exact quantification of the outer wall Be source is therefore currently not possible, but a lower estimate can be obtained by assuming the same erosion rate as on the inboard Be cladding over the total outer limiter area ($A_{lim}^{LFS} = 9m^2$) assuming at least similar CXN and residual plasma flux to the inner and outer SOL and ignoring the filamentary transport responsible for the asymmetry. The lower estimate for the total net main chamber source in diverted configuration amounts to $\simeq 21.2g$.

It should be noted, that the long-term samples in the recessed areas are measuring a net-erosion which in the above calculation is assumed to be the result from a static process. But it can't be excluded that the net-erosion is a result of a dynamic process where in certain operational periods also material is deposited, but then stronger re-eroded in another periods depending on the ion and CXN flux impinging on the sample location. By this dynamic mechanism can the actual throughput of Be material be enhanced. Indeed the emission of Be light from recessed W-coated tiles located on the high-field side of the main chamber indicates that this path of deposition/re-erosion exists, but it can't be yet quantified and is a task for further studies when more tile analysis available to close the balance. Secondly, the potential contribution of erosion from the damaged upper dump plate during diverted plasma operation has not been considered. However, initial post-mortem analysis suggests that the contribution from this location is small [14] and can in first approximation be excluded.

5 Overall material migration with the JET-ILW

The current understanding of the material migration in the JET-ILW in divertor configuration can be described as follows (6a): neutral Be and BeD, are eroded by physical sputtering and CAPS, respectively, from the recessed main chamber wall equipped with Be PFCs. Both, Be and BeD, enters the plasma, is dissociated, ionised and transported by SOL-flows towards the inner divertor where significant deposition of Be on W PFCs takes place. Indeed post-mortem analysis revealed the majority of all deposition is found on top the apron of the inner divertor tile 0 and tile 1 which are in all diverted plasmas located in the far-SOL [19]. The total deposition at this location of cold surface temperature ($T_{surf} 373K$) amounts to at least 28g. This marks the first deposition location of material driven by the SOL flow (6b) and indeed the WallDYN code can well reproduce this observation as depicted in fig. 6c. Details about the WallDYN code and the benchmark with JET gas balance results [1] and post-mortem deposition patten [10] can be found in [20]. Further transport from this location is strongly hindered as the local plasma conditions provide not enough energetic deuterons to re-erode the deposited Be, thus the majority of Be just sticks and builds up a Be layer which incorporates the majority of retained fuel. This is different to JET-C and C where chemical erosion and multiple step transport of ten or more re-erosion cycles occurred which moved the deposited C along the vertical

target plate down to the pump duct entrance resulting in a strong net deposition zone of the whole inner divertor target plate in JET-C [10].

The inner strike-line is for the majority of diverted plasmas in the first year of JET-ILW operation located on the vertical target (tile 3) as shown in fig. 6b. The incident Be ion flux is not sufficient to turn this area into a net Be deposition zone, but reflection and energetic sputtering by deuterons and impurities in steady-state conditions and in particular during ELMs takes place [9, 21, 23]. As no Be deposition layer is build-up, the W-coated CFC vertical tiles 1 and 3, close to the campaign-averaged strike-line position, are indeed representing a net W erosion zone as in-situ *WI* spectroscopy revealed and recent post-mortem analysis confirmed [21]. Fig. 7 shows e.g. the emission pattern of (a) *BeII* at $527.1nm$, (b) D_α , and (c) *WI* at $400.9nm$ in the full W divertor recorded simultaneously in the L-mode phase of a monitoring discharge after about 1500 plasma discharges since first plasma with the JET-ILW. The strong *WI* line emission at the inner strike-line and along the vertical W target plate is clearly visible indicating that the area is not covered by a Be deposited layer. The *WI* emission is peaked close to the PFC surface due to the short penetration depth of neutral W in the attached inner and outer divertor leg which is similar to observations made in TEXTOR [30]. However, due to the rough structure of the W-coated CFC also islands with Be deposition can be identified in the net W erosion areas which is analog to observations made in ASDEX Upgrade, W PFCs and C impurities, attributed to surface roughness [31].

Overall, the Be transport to the divertor floor and even more to the remote areas of the pump-duct entrance is vastly (factor 50) reduced with respect to C in JET-C as measurements and associated ERO modelling confirmed [22]. In the case of JET-C, chemical erosion of C was responsible for the multi-step transport which is vastly reduced in JET-ILW due to the energetic threshold for Be sputtering.

Indeed in the JET-ILW, residual C at much lower levels than in JET-C can be found in the inner leg, but C is enhanced with respect to Be at the floor of the divertor as well as in remote areas [21].

Figure 4c

The outer divertor is showing a complete different erosion/deposition pattern with respect to the inner divertor leg. Though a poloidal SOL flow from the outer wall SOL, starting at the stagnation point, down into the outer leg exists, the amount of Be ions arriving in the outer divertor is insufficient to cause net deposition on top of tile 8. Also the vertical target plates (tile 7 and 8) are not affected and show no sign of erosion or significant deposition. Note that the outer strike line was in the first year of operation predominantly positioned on the bulk W divertor (tile 5 in fig. 7b) which is partially explaining the virgin-like conditions of the vertical W target plates. Tile 5 has not yet been analysed post-mortem, but in-situ W sputtering from the incident Be ion flux was observed and it can be assumed that the W surface is pristine [9].

6 Summary

JET equipped with the Be first wall is an ideal test bed for ITER to study beryllium migration paths and verify plasma-surface interaction codes as WallDYN and ERO. In JET

plasmas in divertor configuration is the amount of beryllium eroded in the main chamber (cladding and limiters) and the amount of beryllium deposited in the inner divertor comparable and lie in the range of 21 – 28g considering the currently analysed PFCs and assuming a static main chamber source. This fair balance is confirming the main understanding of the beryllium migration processes in diverted configuration and the beryllium transport in the SOL towards the inner divertor. The absence of chemical erosion in the case of beryllium is inhibiting the multi-step transport (via deposition/erosion steps) seen with carbon and JET-C. This avoids the re-erosion and transport of beryllium deposited on the apron of the inner divertor tungsten PFCs to remote areas and further the accumulation of beryllium in inaccessible areas in the pump ducts or below as observed with carbon in JET-C. Beryllium sticks in less than two interaction steps to the tungsten PFCs.

The primary impurity source in diverted configuration with the JET-ILW is significantly reduced in comparison with JET-C resulting in a reduction in divertor material deposition by more than an order of magnitude [19]. The absence of low energy sputtering of beryllium is responsible for the reduction of the primary source in JET-ILW with respect to JET-C where the erosion of carbon PFCs by thermal neutrals contributed to the source production. The overall low beryllium migration is also consistent with the observed low fuel inventory and dust production with the JET-ILW [9]. However, more divertor and main chamber PFCs need to be analysed before a full balance can be performed.

Acknowledgment This work has been carried out within the framework of the EUROfusion Consortium and has received funding from the European Union’s Horizon 2020 research and innovation programme under grant agreement number 633053. The views and opinions expressed herein do not necessarily reflect those of the European Commission..

References

- [1] S. Brezinsek et al., Nucl. Fus. 53 (2013) 083023
- [2] R.A. Pitts et al., Plasma Phys. Contr. Fus. 47 (2005) B303
- [3] J. Roth et al., J. Nucl. Mater. 390-391 (2009) 1
- [4] A. Kirschner et al., Nucl. Fus. 40 (2000) 989
- [5] K. Schmid et al., J. Nucl. Mater. 415 (2011) S284
- [6] R. Neu et al., J. Nucl. Mater. 438 (2013) S34
- [7] G.F. Matthews et al., J. Nucl. Mater. 438 (2013) S1
- [8] S. Brezinsek et al., J. Nucl. Mater. 438 (2013) S303
- [9] S. Brezinsek et al., J. Nucl. Mater. doi:10.1016/j.jnucmat.2014.12.007
- [10] A. Widdowson et al., Phys. Scr. T159 (2014)014010
- [11] D. Borodin et al., Phys. Scr. T159 (2014) 014057
- [12] S. Brezinsek et al., Nucl. Fus. 54 (2014) 103001
- [13] K. Heinola et al., submitted for J. Nucl. Mater. PSI2014
- [14] A. Baron- Wiechec et al., submitted for J. Nucl. Mater. PSI2014
- [15] K. Krieger et al., J. Nucl. Mater. 438 (2013) S262
- [16] S. Krat et al., J. Nucl. Mater. 456 (2015) 106
- [17] M. Mayer et al., J. Nucl. Mater. 438 (2013) S780
- [18] D. Carallero et al., J. Nucl. Mater. doi:10.1016/j.jnucmat.2014.10.019
- [19] M. Rubel et al. this conference - submitted to NF
- [20] K. Schmid et al. - this conference - submitted to NF
- [21] M. Mayer - private communication - tbp in Physica Scripta
- [22] A. Kirschner et al., J. Nucl. Mater. doi:10.1016/j.jnucmat.2014.10.072
- [23] J. Beal et al., J. Nucl. Mater. doi:10.1016/j.jnucmat.2014.09.069
- [24] P. Petersson et al., J. Nucl. Mater. doi:10.1016/j.jnucmat.2014.12.077
- [25] D. Borodin et al., Phys. Scripta **T145** (2011) 14008
- [26] D. Nishijima et al., Plasma Phys. Control Fusion **50** (2008) 125007
- [27] C. Björkas et al., New J. Physics **11** (2009) 123017
- [28] J. Roth et al., Nucl. Fus. **36** (1996) 1647
- [29] J.W. Coenen et al., Nucl. Fus. **53** (2013) 073043
- [30] S. Brezinsek et al., Phys. Scripta **T145** (2011) 014016
- [31] K. Schmid et al., Nucl. Fus. **50**(2010) 105004

7 Figures

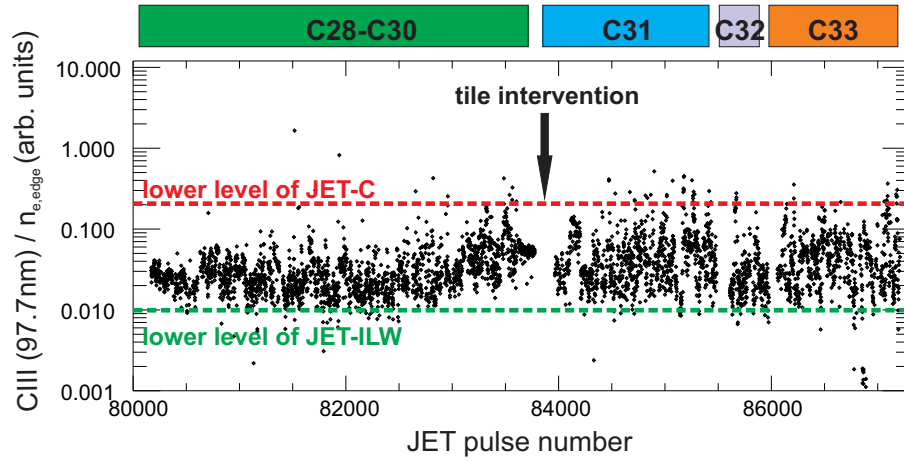


FIG. 1: Carbon content (C_{III}/n_e) in the main chamber plasma edge in JET-C and JET-ILW during the divertor phase of the plasmas as function of discharge number and operational campaign. The lower envelope for the C-content in JET-C and JET-ILW is marked as dashed lines. The period C28-C30 indicated the first year of operation followed by the tile intervention for post-mortem analysis. C31-C33 reflects the second year of JET-ILW operation.

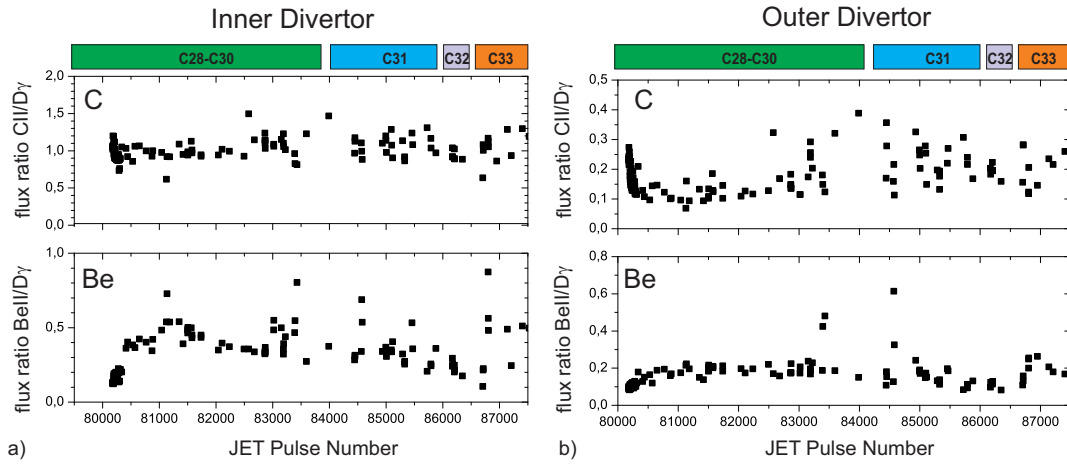


FIG. 2: Development of the C (flux ratio C_{II}/D_{γ}) and Be (flux ratio Be_{II}/D_{γ}) inner divertor (a) and outer divertor content (b) in identical discharges spread of the full period of JET-ILW operation to monitor the Be and C evolution in time. The period C28-C30 indicated the first year of operation followed by the tile intervention for post-mortem analysis. C31-C33 reflects the second year of JET-ILW operation.

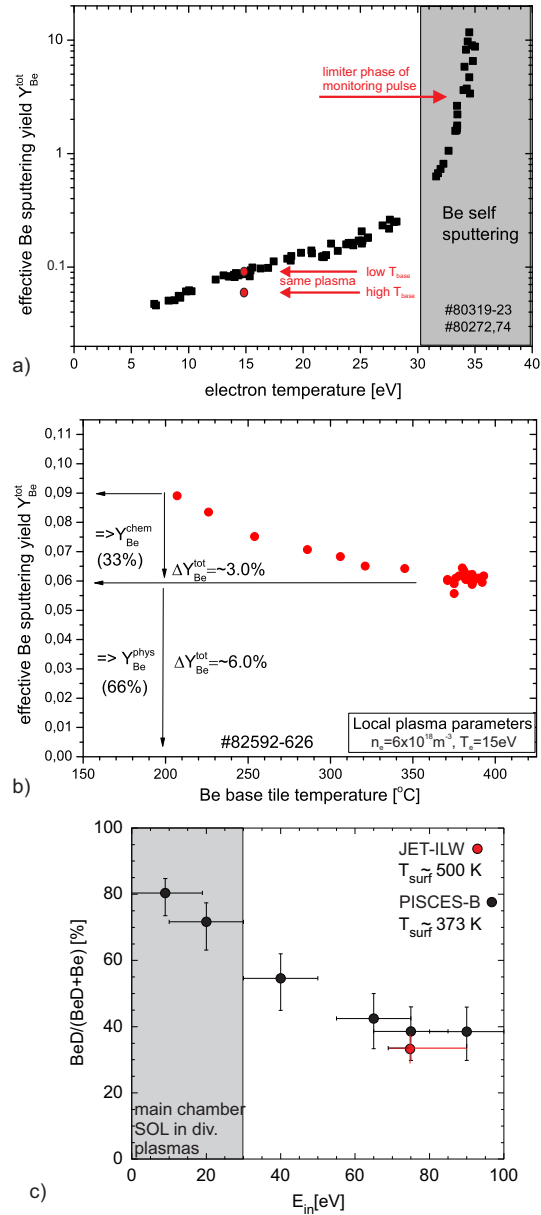


FIG. 3: a) The effective Be sputtering as function of electron temperature, proportional to the impact energy of the impinging ions at almost constant surface temperature. The effective sputtering is determined by deuterons at the lower energy range and Be ions at the higher energy end (shadowed area). b) Composition of the effective Be sputtering yield as function of surface temperature at constant impact energies in a series of identical discharges. c) The normalised contribution of chemical assisted physical sputtering of Be to the total effective Be sputtering yield as function of the impact energies for deuterium ions in PISCES-B and JET-ILW.).

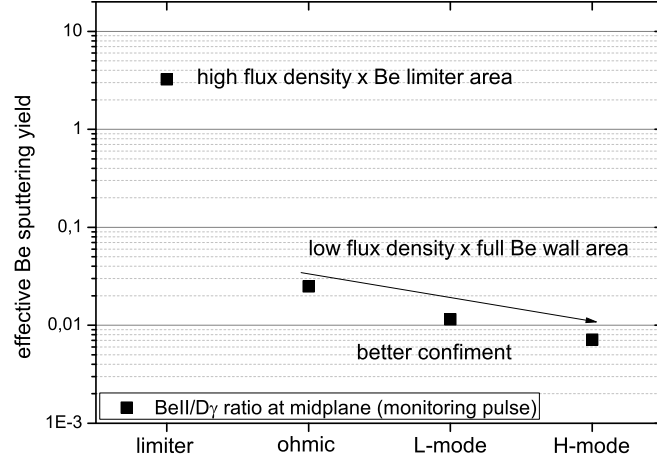


FIG. 4: Typical effective Be sputtering yield in different operational phases (limiter, ohmic, L-mode and H-mode).

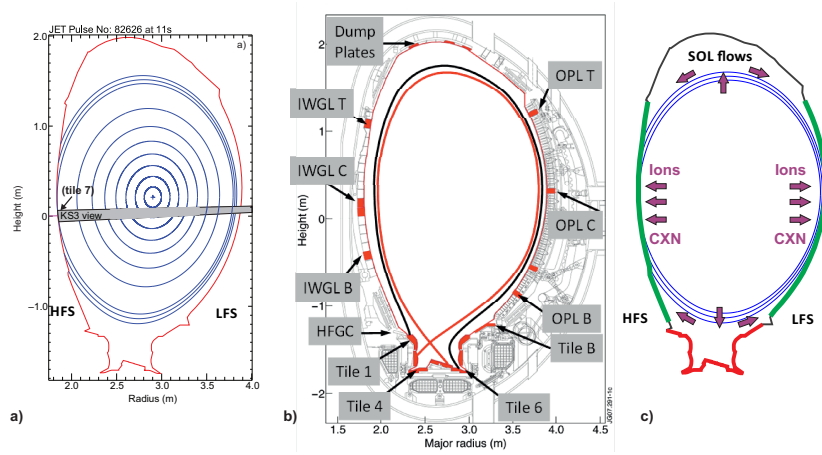


FIG. 5: a) Poloidal cross-section of JET with plasma-facing components extracted and analysed by post-mortem techniques in red. b) Be migration path in limited plasmas. c) Spectroscopic observation chord spotting on the inner wall at the contact point in limited plasmas applied.

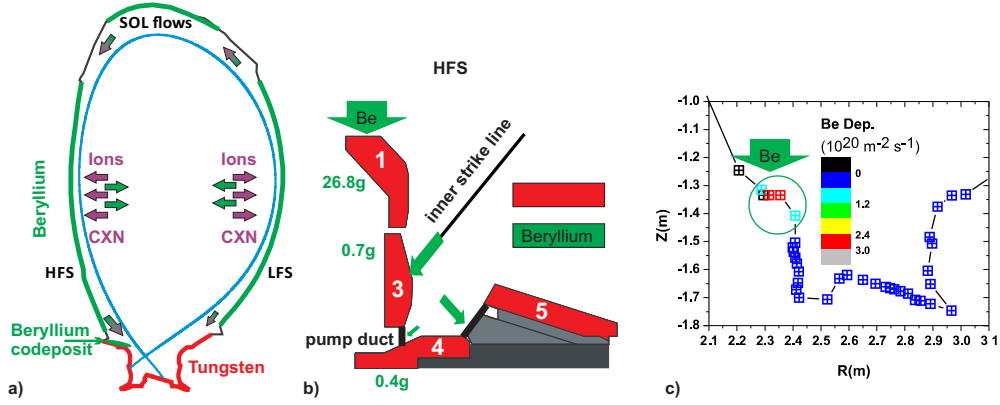


FIG. 6: a) Beryllium migration path in diverted plasmas: from the main chamber into the divertor. b) Material migration within in the inner divertor leg. The Be deposition distribution in g on the inner divertor PFCs. c) WallDYN modelling of an H-mode divertor discharge which shows qualitatively the observed experimental deposition pattern on top of tile 1 [20].

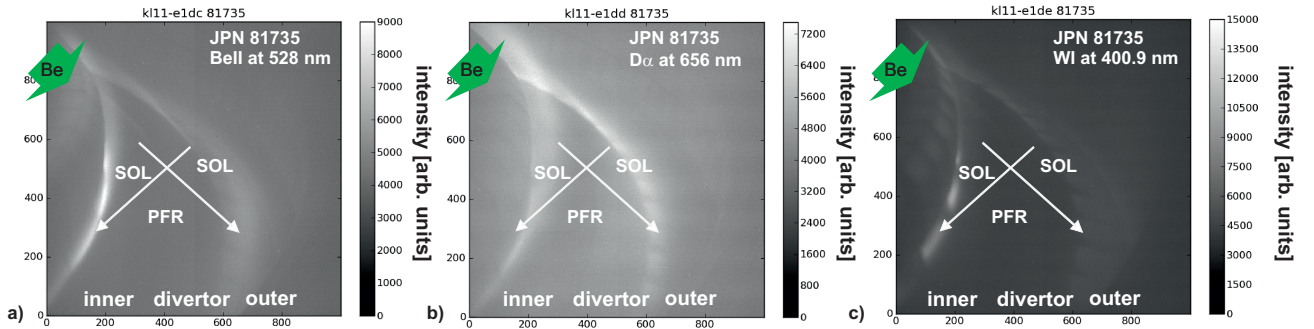


FIG. 7: Emission of a) BeII and b) D_{α} in the divertor during a quiet L mode phase. The inner and outer strike-lines are visible. c) WI light emission in the inner divertor leg showing no WI at top of tile 1 where Be deposits and strong WI along the vertical target with a maximum near the inner strike-line location. The strong emission at the strike-line indicates an intact W surface and no coverage with Be deposit.

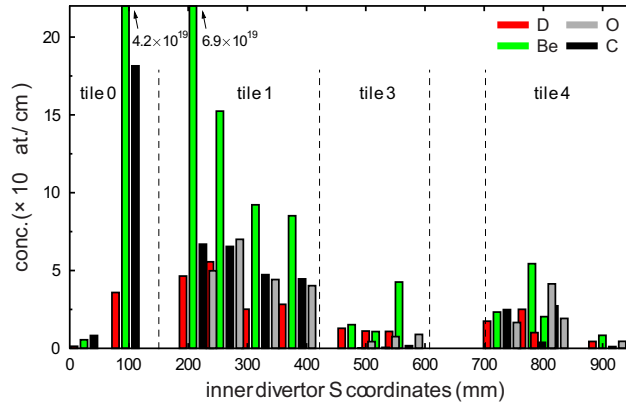


FIG. 8: Beryllium deposition in the inner divertor leg determined post-mortem by ion beam techniques from [13].